HHS Public Access

Author manuscript

Chem Commun (Camb). Author manuscript; available in PMC 2019 December 11.

Published in final edited form as:

Chem Commun (Camb). 2018 December 11; 54(99): 14005–14008. doi:10.1039/c8cc07432a.

Hydrophilic azaspiroalkenes as robust bioorthogonal reporters

Peng An, **Hsuan-Yi Wu**, **Tracey M. Lewandowski**, and **Qing Lin***

Department of Chemistry, State University of New York at Buffalo, Buffalo, New York 14260, USA.

Abstract

Two hydrophilic spiroalkenes, azaspiro[2.3]hex-1-ene and azaspiro[2.4]hept-1-ene, were designed and synthesized. Compared to the previously reported spiro[2.3]hex-1-ene, the azaspiroalkenes exhibited greater water solubility and reactivity as dipolarophiles in the photoindued tetrazale-alkene cycloaddition reaction. In addition, an azaspiro[2.3]hex-1-ene-containing amino acid, AsphK, was found to be charged by an engineered pyrrolysyl-tRNA synthetase into proteins *via* amber codon suppression in *E. coli* as well as in mammalian cells.

Graphical Abstract

Highly strained hydrophilic bioorthogonal reporters, azaspiro[2.3]hex-1-ene and azaspiro[2.4]hept-1-ene, were synthesized and characterized.

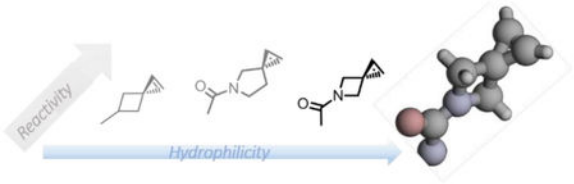

Bioorthogonal chemistry offers a powerful tool to manipulate the biomolecule structure and function in living systems. In this approach, bioorthogonal reporters with a balanced stability and reactivity are introduced into in the biomolecule followed by the bioorthogonal ligation reaction with a biophysical probe.[1] In the design of reactive, *yet* stable, bioorthogonal reporters, the strained ring structures have attracted most attention over the last decade because of their robust reactivity in the catalyst-free bioorthogonal cycloaddition reactions.[2] These include numerous strained alkenes and alkynes such as norbornene,[3] cyclooctyne,[4] *trans*-cyclooctene (TCO),[5] cyclopropene[6] and their derivatives. While significant rate enhancement was observed with these strained molecules, the majority of the strained bioorthogonal reporters are highly lipophilic because of their large hydrocarbon skeleton, which may cause them to interact non-specifically with hydrophobic proteins and as a result, reduce accessibility to their cognate reaction partners.[7] Indeed, several efforts were reported to introduce heteroatoms into the bioorthogonal reporters to reduce overall hydrophobicity

*qinglin@buffalo.edu; Fax: +1 716 6456963; Tel: +1 716 645 4254

Conflicts of interest

There are no conflicts to declare.

with varying degrees of success.[8] Therefore, it is highly desirable to design the hydrophilic strained chemical reporters for robust bioorthogonal cycloaddition reactions.

Previously, we reported the design of spiro[2.3]hex-1-ene (Sph), a highly strained spirocyclic alkene for the photoinduced tetrazole-alkene cycloaddition with k_2 values approaching 10^4 M^{-1} s^{-1} (Fig. 1).[9] An Sph-modified lysine, SphK, was genetically encoded into the class B G protein-coupled receptors (GPCRs) and subsequently labelled with a fluorophore via the tetrazole-alkene cycloaddition reaction.[10] To enhance the utility of Sph as a bioorthogonal reporter, herein we report the design and synthesis of the hydrophilic analogues of Sph by introducing nitrogen into the spirocyclic ring system, structural and kinetic characterizations of the azaspiroalkenes in the photoinduced tetrazole-alkene cycloaddition reaction, and genetic encoding of an azaspirohexene-containing amino acid in bacteria as well as in mammalian cells.

To decrease the hydrophobicity, we considered bioisosteric replacement of carbon with nitrogen in the Sph skeleton. Since amines show pH-dependent charge states, we further designed the amide linkage so that the reporter structure is hydrophilic whose polarity is not pH dependent. Accordingly, three Sph derivatives were designed with the difference being the second spirocyclic ring size (Fig. 1). The calculated cLogP values for the three spiroalkenes **1**–**3** are −0.64, −0.37, and −0.66, respectively, all of which are significantly lower than that of Sph (Fig. 1). On their reactivity, the calculated LUMO energies of the azaspiroalkenes were lower than that of SphK, leading to the reduced HOMO−LUMO gap and likely higher cycloaddition rate with the in situ generated nitrile imines.[11]

For the synthesis of azaspiroalkenes **1**-**3**, synthetic routes analogous to Sph were adopted (Scheme 1). For azaspirohexene (**1**), the commercially available starting materials, *N*-Boc-3-oxoazetidine, was transformed into the exocyclic alkene **1a** in 65% yield via the Wittig reaction. After switching the protecting group from Boc to methoxy-trityl group, the spirocycle **1c** was obtained in 71% yield through dibromo carbene insertion in the presence of 50% NaOH solution. Subsequent $Ti(O^iPr)_4$ catalysed mono-debromination by EtMgBr followed by KO^tBu mediated elimination of HBr produced the methoxy-trityl protected azaspirohexene **1e**. Removal of the trityl group followed by acetylation by acetyl chloride afforded azaspirohexene **1** in 83% yield (Scheme 1a). For synthesis of azaspiroheptene **2**, the commercially available *N*-Noc-3-oxopyrrolidine was used as the starting materials. An identical route was taken except that the trityl protecting group was used during the cyclopropanation, debromonation, and elimination reactions (Scheme 1b). For the synthesis of azaspiro[2.2]hep-1-ene, the key intermediate, dibromo-azaspiropentane **3d**, was obtained in 60% yield after carbene insertion into the reported structure **3c**[12] (Scheme 1c). However, repeated attempts to convert **3d** to spiropentene **3** were not successful, presumably due to the high ring strain present in such a small spirocyclic system. Moreover, spirocycle **3d** decomposed gradually in solution at room temperature. Nevertheless, TLC analysis indicated that azaspirohexene **1** is indeed much more polar than the corresponding spirohexene (Table S1 in ESI). In addition, LC-MS-based measurements gave Log*P* values of −0.95 and −0.12 for azaspiroalkenes **1** and **2**, respectively, lower than that of an acetal-substituted Sph (Log*P* = 0.13; Table S2 in ESI), indicating that the azaspiroalkenes are indeed more hydrophilic than spirohexene.

The reactivity of 3,3-disubstituted cyclopropenes, to which spiroalkenes belong, in the cycloaddition reactions are known to be critically dependent on the steric hindrance.[9,13] For the nitrile imine-mediated 1,3-dipole cycloaddition, the reduced bond angle between two C^3-substituents leads to lower steric hindrance and thus higher reactivity.[9] To determine how the nitrogen replacement affects the bond angle, we prepared an azaspiro[2.3]hex-1-ene derivative **1f** (Scheme 1a) and obtained its crystal structure (Table S2 in ESI). Compared to the Sph structure, the basic framework of azaspirohexene (Asph) stays intact with some minor changes (Fig. 2). For example, the bond angle between the two C^3-substituents in Asph is 90.7°, smaller than 92.3° of Sph,[9] suggesting somewhat reduced steric hindrance compared to Sph. The double-bond length in the cyclopropene ring of Asph is longer than that of Sph (1.292 Å vs. 1.268 Å; Fig. 2), indicating that the π-bond is weaker and potentially more reactive in the cycloaddition reaction.

To determine the reactivity experimentally, we carried out the kinetics analysis of spiroalkenes **1**, **2** and Sph in the cycloaddition reaction with two tetrazoles, **Tet-1** and **Tet-2**,[10] and the results are collected in Table 1. Because the cycloaddition produces fluorescent pyrazoline adduct, we followed the reaction progress by monitoring time-dependent fluorescence increases (Fig. S1–S6 in ESI). All reactions proceeded fast, with the second-order rate constant, k_2, exceeding 10^4 M^{-1} s^{-1}. In particular, azaspiro[2.4]hept-1-ene **2** gave the fastest reaction, with k_2 value of 3.32×10^4 M^{-1} s^{-1} (Table 1). For the sterically less hindered **Tet-1**, azaspiroalkenes **1** and **2** reacted faster than Sph (compare entries 2 and 3 to 1 in Table 1), in agreement with their lower LUMO energies (Fig. 1). For the sterically shielded **Tet-2**,[10] the reactivity enhancement is negligible, suggesting that the small changes in bond angle and bond length, as observed for Asph in Fig. 2, have no effect on lowering the transition state energy. The NMR studies of the cycloaddition reaction at higher mM concentrations between **Tet-1** and spiroalkene **1** or **2** showed about 90~95% conversion after 2-hour photoirradiation (Fig. S7–S8 in ESI).

To assess the stability of azaspiroalkenes **1** and **2** in biological milieu, we incubated azaspiroalkenes with excess amount of reduced glutathione (GSH; 10 mM) for one week and found them to be stable in mixed DMSO/PBS (3:1) solvent for one week at room temperature based on ^{1}H NMR (Fig. S9–S10 in ESI). Considering their excellent water-solubility, robust stability, and enhanced reactivity, we synthesized the azaspirohexene-conjugated lysine, AsphK (Scheme S4 in ESI), which unlike SphK turned out to be completely water-soluble. We then screened a panel of pyrrolysyl-tRNA synthetase (PylRS) variants[14] for their ability to charge AsphK into superfolder green fluorescent protein containing amber codon at position-204 (sfGFP-204TAG) in *E. coli*. To our delight, we found a PylRS variant previously reported to charge TCOK, or TCOKRS,[7] supported site-specific incorporation of AsphK into sfGFP-204TAG with expression yield of 0.1 mg/L (Fig. S11 in ESI), which is significant lower than that of the SphK-encoded sfGFP mutant (4.9 mg/L) catalysed by the wild-type PylRS.[9] We then compared the reactivity of AsphK to SphK in the protein context with a Cy5-conjugated tetrazole we used previously[10] (Fig. 3a), and found that AsphK gave higher amount of the labelling product based on Cy5 fluorescence intensity (Fig. 3b), along with several minor, faster-migrating bands probably generated as a result of the degradation of the AsphK-encoded sfGFP protein. Because Asph

showed a similar reactivity compared to Sph in the kinetic study (compare entry 5 to 4 in Table 1), we attributed this reactivity enhancement to the greater accessibility of AsphK in aqueous medium because of its hydrophilicity. Indeed, improve solvent accessibility of bioorthogonal reporters has been shown to be responsible for higher labeling yields.[15]

To probe whether Asph can be incorporated site-specifically into proteins in mammalian cells, we co-transfected human embryonic kidney (HEK) 293T cells (obtained from ATCC) with two plasmids, one encoding TCOKRS and *t*RNAPyl CUA, and the other encoding a fluorescent mCherry-EGFP reporter containing a TAG amber codon in the middle and an HA-tag at C-terminus (Fig. 4a). Cells were grown in DMEM medium supplemented with 10% FBS in the absence or presence of 1 mM AsphK for 48 h, and imaged by a fluorescent microscope. The EGFP fluorescence was detected only when AsphK was present in the medium (Fig. 3b, Fig. S12). The anti-HA western blot of the cell lysates confirmed the expression of full-length mCherry-EGFP-HA fusion protein when AsphK was present, although a low-level background suppression was also detected when AsphK was absent (Fig. 3c), which can be attributed to the promiscuity of TCOKRS.[16]

In conclusion, we have designed and synthesized two novel spiroalkene bioorthogonal reporters, azaspiro[2.3]hex-1-ene and azaspiro[2.4]hept-1-ene. Compared to the carbocyclic Sph, the azaspiroalkenes are water-soluble and exhibit improved kinetics with k_2 values approaching $3.32 \times 10^4\ M^{-1}\ s^{-1}$ in the photoinduced tetrazole-alkene cycloaddition reaction. Moreover, a lysine derivative containing the azaspiro[2.3]hex-1-ene reporter (AsphK) was incorporated into sfGFP site-specifically *via* amber codon suppression. The AsphK-encoded sfGFP was labelled at a higher efficiency than the SphK-encoded counterpart presumably due to its greater accessibility in aqueous medium. Finally, the incorporation of AsphK into a reporter protein in mammalian cells was demonstrated. Because of its hydrophilicity and robust reactivity, Asph could find wide use in bioorthogonal studies of biomolecular structure, dynamics and function in living systems.

Supplementary Material

Refer to Web version on PubMed Central for supplementary material.

Acknowledgements

We gratefully acknowledge NIH (GM085092) for financial support. We thank Jordan Cox at SUNY Buffalo for solving X-ray structure for compound **1f** with Cambridge Structural Database accession number: CCDC 1864586.

Notes and references

1. Sletten EM and Bertozzi CR, Angew. Chem., Int. Ed, 2009, 48, 6974;Lim RKV and Lin Q, Chem. Commun, 2010, 46, 1589;Ramil CP, Q. Lin, Chem. Commun 2013, 49, 11007;Lang K and Chin JW, Chem. Rev 2014, 114, 4764; [PubMed: 24655057] Patterson DM, Nazarova LA and Prescher JA, ACS Chem. Biol 2014, 9, 592–605; [PubMed: 24437719] Oliveira BL, Guo Z and Bernardes GJL, Chem. Soc. Rev 2017, 46, 4895. [PubMed: 28660957]
2. Debets MF, Berkel SSV, Dommerholt J, Dirks AJ, Rutjes FPJT, and Delft FLV, Acc. Chem. Res, 2011, 44, 805; [PubMed: 21766804] Liu F, Liang Y and Houk KN, Acc. Chem. Res, 2017, 50, 2297. [PubMed: 28876890]

3. Han H-S, Devaraj NK, Lee J, Hilderbrand SA, Weissleder R and Bawendi MG, J. Am. Chem. Soc 2010, 132, 7838; [PubMed: 20481508] van Berkel SS, Dirks AJ, Debets MF, van Delft FL, Cornelissen JJLM, Nolte RJM and Rutjes FPJT, ChemBioChem 2007, 8, 1504; [PubMed: 17631666] Devaraj NK, Weissleder R, Hilderbrand SA, Bioconjugate Chem 2008, 19, 2297.
4. Agard NJ, Prescher JA and Bertozzi CR, J. Am. Chem. Soc 2004, 126, 15046. [PubMed: 15547999]
5. Blackman ML, Royzen M and Fox JM, J. Am. Chem. Soc 2008, 130, 13518; [PubMed: 18798613]
6. Yang J, Šečkutė J, Cole CM and Devaraj NK, Angew. Chem., Int. Ed 2012, 51, 7476;Patterson DM, Nazarova LA, Xie B, Kamber DN and Prescher JA, J. Am. Chem. Soc 2012, 134, 18638; [PubMed: 23072583] Yu Z, Pan Y, Wang Z, Wang J and Lin Q Angew. Chem., Int. Ed 2012, 51, 10600.Ramil CP, Dong M, An P, Lewandowski TM, Yu Z, Miller LJ and Lin QJ Am. Chem. Soc 2017, 139, 13376.
7. Lang K, Davis L, Wallace S, Mahesh M, Cox DJ, Blackman ML, Fox JM and Chin JW, J. Am. Chem. Soc 2012, 134, 10317; [PubMed: 22694658] Nikic I, Plass T, Schraidt O, Szyman ski J, Briggs JAG, Schultz C and Lemke EA, Angew. Chem. Int. Ed 2014, 53, 2245;Uttamapinant C, Howe JD, Lang K, Beránek V, Davis L, Mahesh M, Barry NP and Chin JW, J. Am. Chem. Soc 2015, 137, 4602. [PubMed: 25831022]
8. Engelsma SB, Willems LI, van Passchen CE, van Kasteren SI, van der Marel GA, Overkleeft HS and Filippov DV, Org. Lett 2014, 16, 2744; [PubMed: 24796604] Kozma E, Nikić I, Varga BR, Aramburu IV, Kang JH, Fackler OT, Lemke EA and Kele P, ChemBioChem 2016, 17, 1518; [PubMed: 27223658] Siegl SJ, Vázquez A, Dzijak R, Dračínský M, Galeta J, Rampmaier R, Klepetářová B and Vrabel M, Chem. Eur. J 2018, 24, 2426. [PubMed: 29243853]
9. Yu Z and Lin Q, J. Am. Chem. Soc, 2014, 136, 4153. [PubMed: 24592808]
10. An P, Lewandowski TM, Erbay TG, Liu P and Lin Q, J. Am. Chem. Soc, 2018, 140, 4860. [PubMed: 29565582]
11. Wang Y, Song W, Hu WL and Lin Q, Angew. Chem., Int. Ed, 2009, 48, 5330;An P and Lin Q, Org. Biomol. Chem, 2018, 16, 5241. [PubMed: 29995029]
12. Ince J, Ross TM, Shipman M and Slawin AMZ, Tetrahedron, 1996, 52, 7037.
13. Kamber DN, Nazarova LA, Liang Y, Lopez SA, Patterson DM, Shih H-W, Houk KN, Prescher JA, J. Am. Chem. Soc 2013, 135, 13680. [PubMed: 24000889]
14. Wan W, Tharp JM and Liu WR, Biochim. Biophys. Acta, 2014, 1844, 1059. [PubMed: 24631543]
15. Rahim MK, Kota R, and Haun JB, Bioconjugate Chem 2015, 26, 352.
16. Shang X, Song X, Faller C, Lai R, Li H, Cerny R, Niu W and Guo J, Chem. Sci 2017, 8, 1141. [PubMed: 28451254]

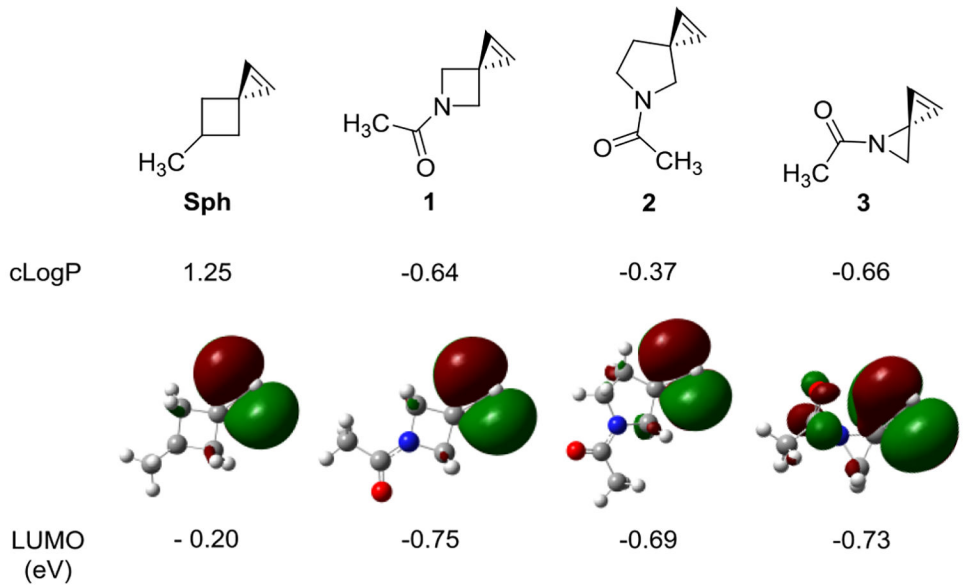

Fig. 1.

Structures of spiro[2.3]hex-1-ene and its aza derivatives with their cLogP values, optimized geometries, and LUMO energies shown below the structure. The LUMO energies were calculated using the B3LYP method at 6–31++G** level in vacuum at 298 K.

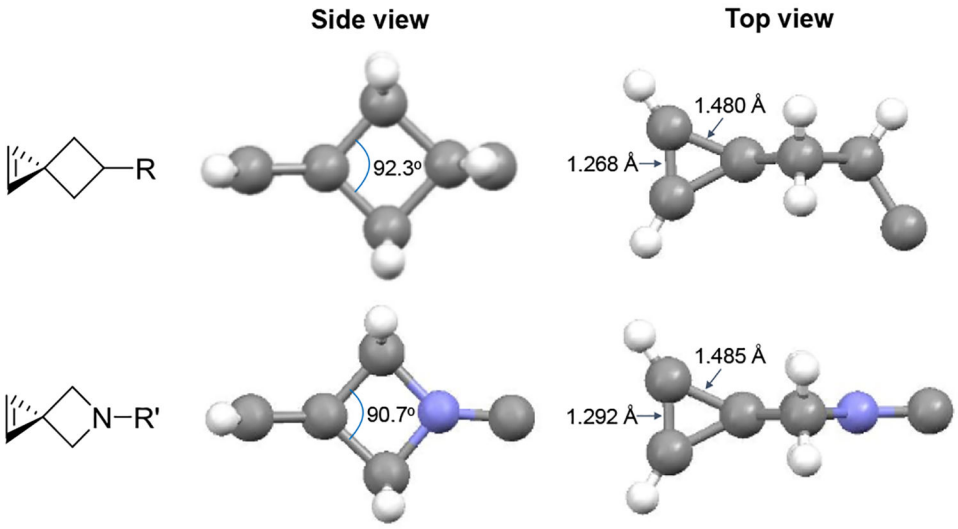

Fig. 2.

Crystal structures of the spirohexene (top) and azaspirohexene **1f** (bottom) viewed from the side and the top. The R or R' group are omitted for clarity.

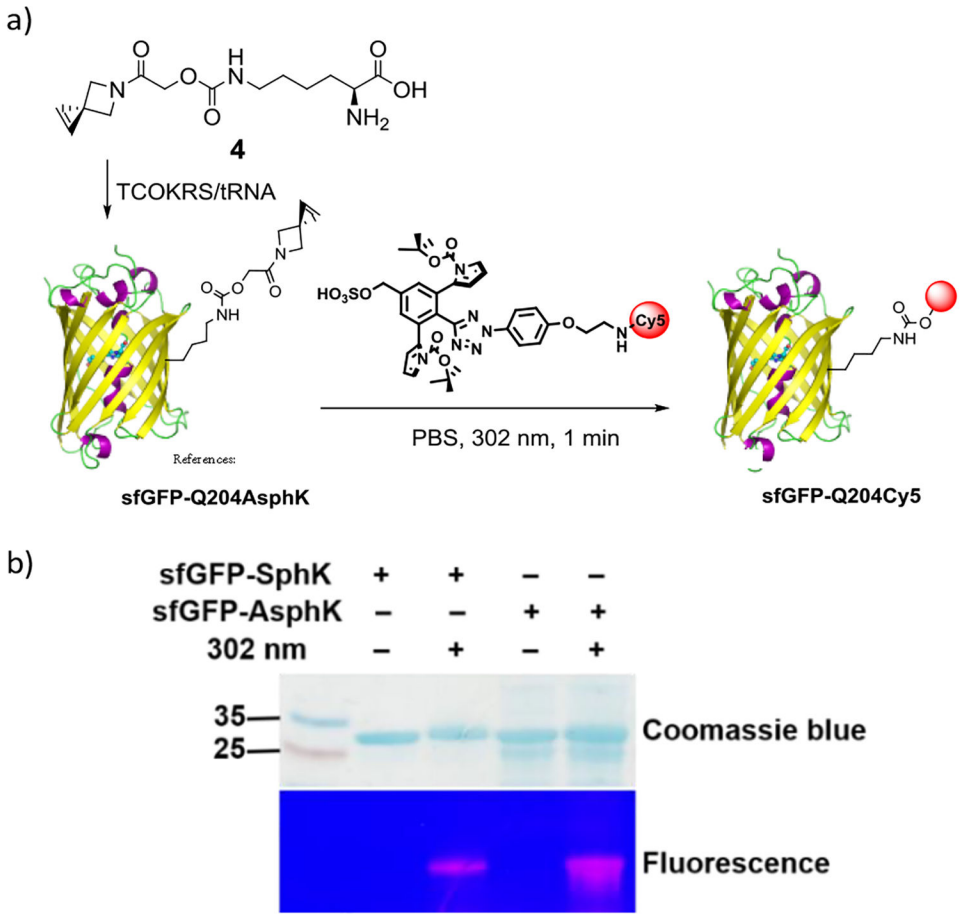

Fig. 3.

Fluorescent labelling the AsphK-encoded sfGFP with a Cy5-conjugated sterically shielded tetrazole. (**a**) Reaction scheme. (**b**) SDS-PAGE analysis of the reaction mixture after irradiating the solution of sfGFP-Q204SphK/sfGFP-Q204AsphK and Cy5-conjugated tetrazole (100 μM) in PBS with a 302-nm UV lamp for 1 min. Top panel, Coomassie blue stained gel; bottom panel, in-gel fluorescence analysis by illuminating the same gel with 365-nm UV light.

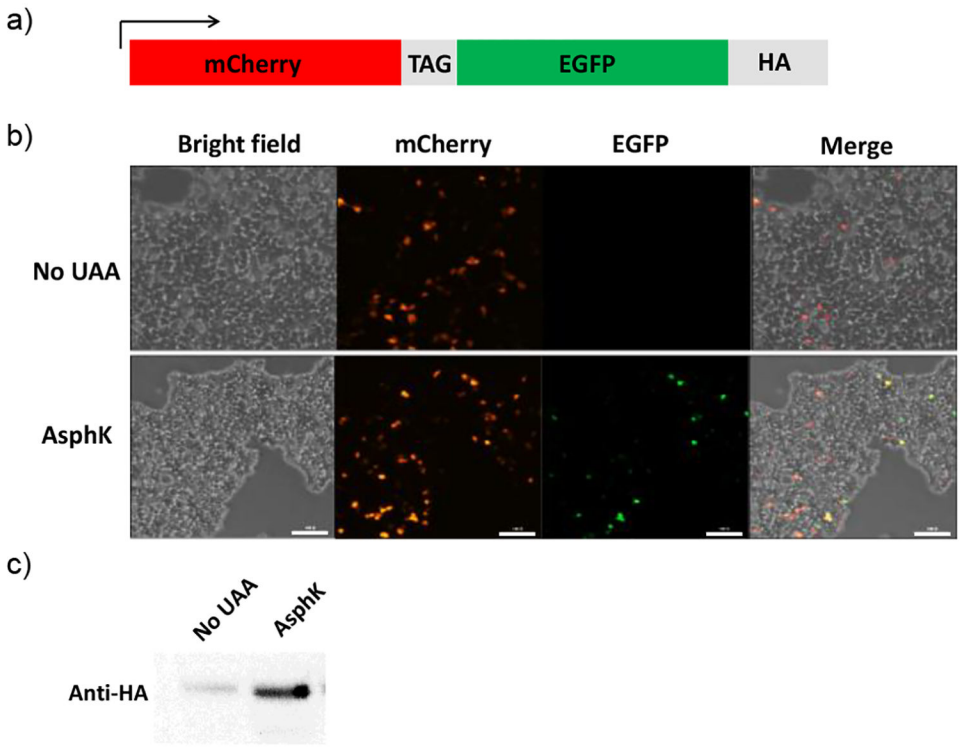

Fig. 4.

Genetic encoding of AsphK in mammalian cells. (**a**) Structural diagram of the mCherry-TAG-EGFP-HA reporter. (**b**) Bright field and fluorescent micrographs of HEK 293T cells transfected with plasmids encoding mCherry-TAG-EGFP-HA and TCOKRS/*t*RNAPyl CUA and cultured in DMEM medium supplemented with 10% FBS in the absence or presence of 1 mM AsphK. Scale bar = 1000 μm. (c) Western blot analysis of HEK 293T cell lysates probed with anti-HA antibody.

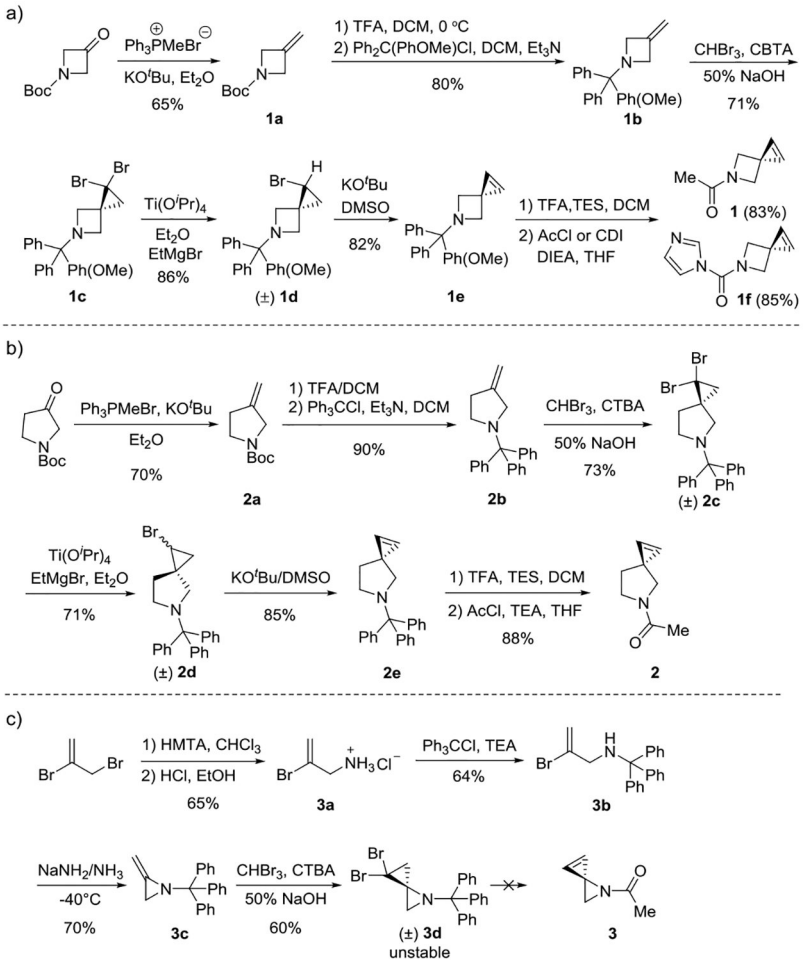

Scheme 1.
Synthesis of the spiroalkenes.

Table 1

Kinetic characterization of the cycloaddition reactions between spiroalkenes and tetrazoles[a]

Tet-1, R=H
Tet-2, R=2-Boc-pyrrole

entry	spiroalkene	tetrazole	k_2 (M^{-1} s^{-1})
1	Sph	**Tet-1**	15,200 ± 3,500
2	**1**	**Tet-1**	22,400 ± 7,500
3	**2**	**Tet-1**	33,200 ± 5,500
4	Sph	**Tet-2**	13,200 ± 1,100
5	**1**	**Tet-2**	14,100 ± 2,200
6	**2**	**Tet-2**	17,000 ± 3,500

[a]A solution of tetrazole (1 μM) and spiroalkene (10 μM) in PB/ACN (1:1), pH = 7.4, in a quartz cuvette was photoirradiated with a 302-nm UV lamp for various times prior to fluorescence measurement. PB = phosphate buffer, ACN = acetonitrile. The formation of the pyrazoline adducts was confirmed by mass spectrometry.